

Reactions of Laser-Ablated Nb and Ta Atoms with N₂: Experimental and Theoretical Study of M(NN)_x (M = Nb, Ta; x = 1–4) in Solid Neon

Zhang-Hui Lu,^{‡,‡} Ling Jiang,[†] and Qiang Xu^{*,†,†}

National Institute of Advanced Industrial Science and Technology (AIST), Ikeda, Osaka 563-8577, Japan, and Graduate School of Engineering, Kobe University, Nada Ku, Kobe, Hyogo 657-8501, Japan

Received: April 5, 2010; Revised Manuscript Received: May 17, 2010

Reactions of laser-ablated niobium and tantalum atoms with dinitrogen in solid neon have been investigated using matrix-isolation infrared spectroscopy. The Nb(NN)_x and Ta(NN)_x (x = 1–4) molecules formed during sample deposition or on annealing are the major products. The products are characterized on the basis of isotopic shifts, mixed isotopic splitting patterns, stepwise annealing, and change of reagent concentration and laser energy. Density functional theory calculations have been performed to understand the structures, ground electronic states, and bonding characteristics of niobium and tantalum dinitrogen complexes. The overall agreement between the experimental and calculated vibrational frequencies, relative absorption intensities, and isotopic shifts supports the identification of these species from the matrix infrared spectra. The molecular orbital analyses and plausible reaction pathways for the formation of the products are also discussed.

Introduction

Dinitrogen fixation and activation are one of the most challenging and important subjects in chemistry. The interaction of dinitrogen with metal atoms is of considerable interest from an academic or an industrial viewpoint owing to its importance in biological and catalytic systems.^{1–3} Since the discovery of the first dinitrogen complex [Ru(NH₃)₅(N₂)]²⁺ in 1965,⁴ the synthesis, structural characterization, and reactivity of metal dinitrogen complexes have been the subject of intensive studies, and a series of metal dinitrogen complexes have been experimentally and theoretically characterized.⁵ Taking the group 5 metal dinitrogen complexes as an example, neutral V(NN)_n (n = 1, 2, 4, 6),⁷ Nb(NN)_n, and Ta(NN)_n (n = 1, 4, 6)⁸ complexes have been reported in excess argon and pure nitrogen. Electron-spin resonance spectroscopy has been applied to neutral V(NN)₆ and Nb(NN)₆ complexes in pure solid nitrogen.⁹ Recently, the gas-phase metal ion complexes V⁺(N₂)_n (n = 3–7)¹⁰ and Nb⁺(N₂)_n (n = 3–16)¹¹ have been generated in a pulsed nozzle laser vaporization source and investigated via infrared photodissociation spectroscopy. Avenier and co-workers have studied the activation of dinitrogen by an isolated surface Ta atom.¹² In addition, various groups have studied the molecular adsorption of N₂ onto group 5 metal clusters and surfaces.¹³ To supplement the experimental work on these systems, ab initio methods and density functional theory (DFT) have been performed to understand the electronic structures and bonding characteristics.^{7–13}

Recent studies have shown that, with the aid of isotopic substitution, matrix isolation infrared spectroscopy combined with DFT calculation is very powerful in investigating the spectrum, structure, and bonding of novel species and the related reaction mechanisms.^{14–16} Various metal dinitrogen complexes have been prepared in low-temperature matrix samples by codeposition of laser-ablated transition-metal and main-group-

element atoms with N₂.⁵ Absorptions at 1965.2 and 1947.6 cm⁻¹ were tentatively assigned to the stretching frequencies of Nb(NN) and Ta(NN) in pure nitrogen.^{8a} The Nb(NN)₄ and Ta(NN)₄ molecules were characterized from isotope experiments in pure nitrogen and excess argon without theoretical calculation.^{8a} However, much less is known about the M(NN)_{2–3} (M = Nb, Ta) molecules. To gain insight into the whole series of niobium and tantalum dinitrogen complexes, we investigated the structures, ground electronic states, and bonding characteristics of niobium and tantalum dinitrogen complexes by probing the N–N vibration in reaction products with IR spectroscopy and DFT calculations. Considering that solid neon may stabilize some species that are difficult to observe in solid argon,¹⁴ we have performed the reactions of laser-ablated niobium and tantalum atoms with N₂ molecules in excess neon, which provides obvious evidence for the formation of the M(NN)_x (M = Nb, Ta; x = 1–4) molecules.

Experimental and Theoretical Methods

The experiments for laser ablation and matrix isolation infrared spectroscopy are similar to those previously reported.¹⁷ In short, the Nd:YAG laser fundamental (1064 nm, 10 Hz repetition rate with 10 ns pulse width) was focused on the rotating Nb and Ta targets. The laser-ablated Nb and Ta atoms were co-deposited with N₂ (99.95%, Suzuki Shokan Co., Ltd.) in excess neon onto a CsI window cooled normally to 4 K by means of a closed-cycle helium refrigerator. Typically, 5–25 mJ/pulse laser power was used. Isotopic ¹⁵N₂ (99.8%, Shoko Co., Ltd.) and ¹⁴N₂ + ¹⁵N₂ mixtures were used in different experiments. In general, matrix samples were deposited for 30–60 min with a typical rate of 2–4 mmol per hour. After sample deposition, IR spectra were recorded on a Bio-Rad FTS-6000e spectrometer at 0.5 cm⁻¹ resolution using a liquid-nitrogen-cooled HgCdTe (MCT) detector for the spectral range of 5000–400 cm⁻¹. Samples were annealed at different temperatures and subjected to broad-band irradiation (λ > 250 nm) using a high-pressure mercury arc lamp (Ushio, 100 W).

DFT calculations were performed to predict the structures and vibrational frequencies of the observed reaction products

* To whom correspondence should be addressed. E-mail: q.xu@aist.go.jp.

[†] National Institute of Advanced Industrial Science and Technology (AIST).

[‡] Kobe University.

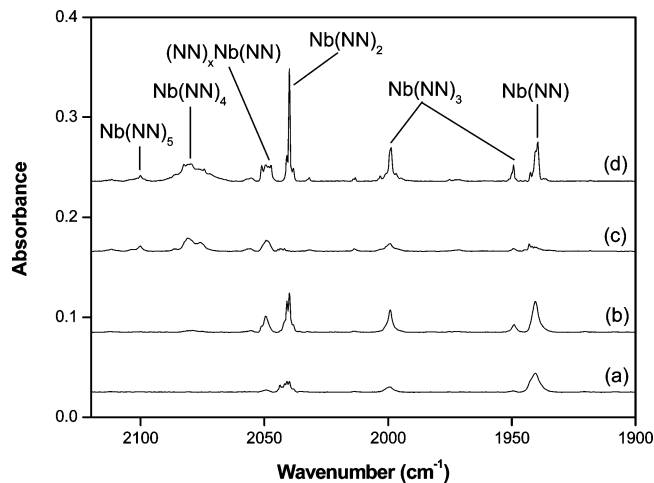


Figure 1. Infrared spectra in the 2120–1900 cm^{-1} regions from codeposition of laser-ablated Nb atoms with 0.3% N_2 in Ne at 4 K. (a) Spectrum obtained from initial deposited sample for 30 min, (b) spectrum after annealing to 8 K, (c) spectrum after 10 min of broad-band irradiation, and (e) spectrum after annealing to 10 K.

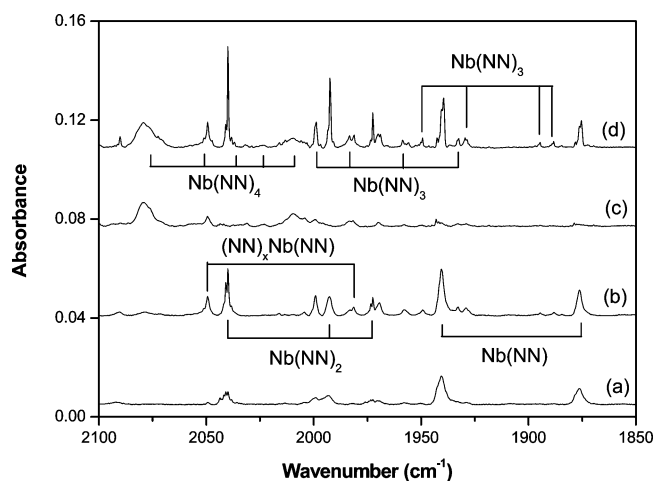


Figure 2. Infrared spectra in the 2100–1850 cm^{-1} region from codeposition of laser-ablated Nb atoms with 0.2% $^{14}\text{N}_2$ + 0.2% $^{15}\text{N}_2$ in Ne at 4 K. (a) Spectrum obtained from initial deposited sample for 30 min, (b) spectrum after annealing to 8 K, (c) spectrum after 10 min of broad-band irradiation, and (e) spectrum after annealing to 10 K.

using the Gaussian 03 program.¹⁸ The B3LYP density functional method was utilized.¹⁹ The 6-311+G(d) basis set was used for the N atoms,²⁰ and the Los Alamos effective-core-potential plus double- ζ (LANL2DZ) basis set was used for the Nb and Ta atoms.²¹ All geometrical parameters were fully optimized, and the harmonic vibrational frequencies were calculated with analytical second derivatives. Trial calculations and recent investigations have shown that such computational methods can provide reliable information for metal complexes, such as infrared frequencies, relative absorption intensities, and isotopic shifts.^{15–17,22–24}

Results and Discussion

Experiments have been done with N_2 concentrations ranging from 0.05% to 1.0% in excess neon. Typical infrared spectra for the products in the selected regions are illustrated in Figures 1–4, and the absorption bands in different isotopic experiments are listed in Table 1. These bands are observed in lower laser power experiments and not favored with higher laser energy and low N_2 concentration, suggesting that one metal atom is

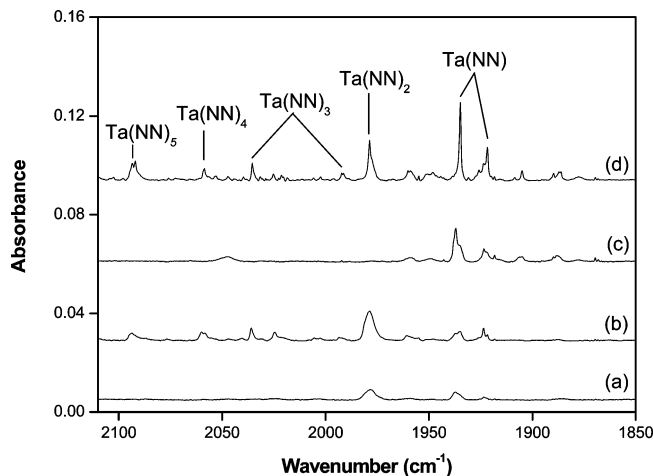


Figure 3. Infrared spectra in the 2110–1850 cm^{-1} regions from codeposition of laser-ablated Ta atoms with 0.08% N_2 in Ne at 4 K. (a) Spectrum obtained from initial deposited sample for 30 min, (b) spectrum after annealing to 8 K, (c) spectrum after 10 min of broad-band irradiation, and (e) spectrum after annealing to 10 K.

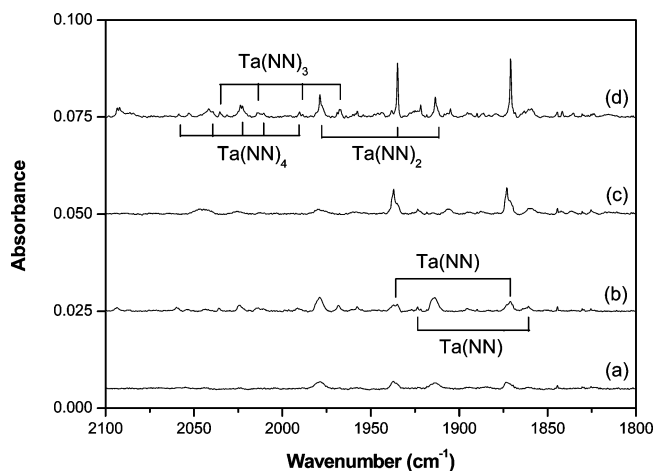


Figure 4. Infrared spectra in the 2100–1850 cm^{-1} region from codeposition of laser-ablated Ta atoms with 0.08% $^{14}\text{N}_2$ + 0.08% $^{15}\text{N}_2$ in Ne at 4 K. (a) Spectrum obtained from initial deposited sample for 30 min, (b) spectrum after annealing to 8 K, (c) spectrum after 10 min of broad-band irradiation, and (e) spectrum after annealing to 10 K.

involved. Doping with CCl_4 has no effect on these bands, which suggests that the reactions products are neutral. The stepwise annealing and photolysis behavior of the product absorptions is also shown in the figures and will be discussed below.

Density functional theory calculations have been carried out for the possible isomers and electronic states of the potential product molecules. Figure 5 shows the ground state structures of the products. Table 2 reports a comparison of the observed and calculated IR frequencies and isotopic frequency ratios for the N–N stretching modes of the observed products. Energetic analysis for possible reactions of Nb and Ta atoms with N_2 is given in Table 3. Due to the similarity of the bonding mechanism between the two series of niobium and tantalum dinitrogen complexes, molecular orbital depictions of the highest occupied molecular orbitals (HOMOs) and HOMO-1s of the representative $\text{Nb}(\text{NN})_x$ ($x = 1–4$) complexes are illustrated in Figure 6.

M(NN). In the Nb + N_2 experiments, the absorption at 1939.5 cm^{-1} appears during sample deposition, increases upon sample annealing, visibly decreases after broad-band irradiation, and recovers after further annealing to higher temperature (Table 1

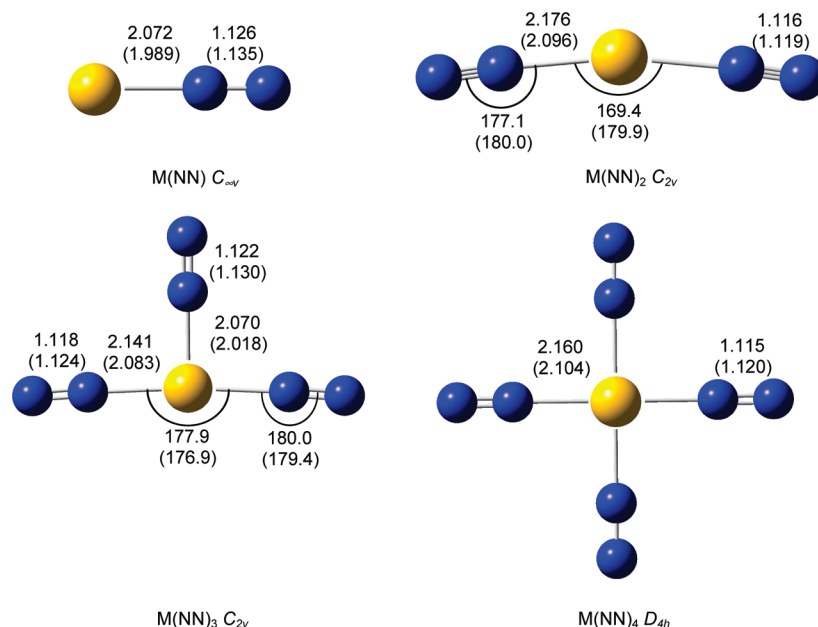


Figure 5. Optimized structures (bond lengths in angstroms, bond angles in degrees) of the niobium and tantalum (in parentheses) dinitrogen complexes calculated at the B3LYP/6-311+G(d)-LANL2DZ level.

TABLE 1: IR Absorptions (in cm^{-1}) Observed from Reaction of Laser-Ablated Nb and Ta Atoms with N_2 in Excess Neon

$^{14}\text{N}_2$	$^{15}\text{N}_2$	$^{14}\text{N}_2 + ^{15}\text{N}_2$	$^{14}\text{N}_2/^{15}\text{N}_2$	assignment
Niobium				
2149.4	2078.3		1.0342	Nb(NN) ₆ site
2130.0	2059.5		1.0342	Nb(NN) ₆
2100.1	2030.5		1.0343	Nb(NN) ₅
2079.4	2010.8	2079.4, 2051.0, 2036.9, 2023.2, 2009.4	1.0341	Nb(NN) ₄
2049.4	1981.4		1.0343	(NN) ₂ Nb(NN)
2039.9	1972.4	2039.9, 1992.4, 1972.4	1.0342	Nb(NN) ₂
1998.8	1932.6	1998.8, 1983.3, 1958.6, 1932.5	1.0343	Nb(NN) ₃
1949.3	1884.6	1949.3, 1929.5, 1894.4, 1884.6	1.0343	Nb(NN) ₃
1939.5	1875.5	1939.5, 1875.3	1.0341	Nb(NN)
Tantalum				
2110.0	2039.5		1.0346	Ta(NN) ₆
2092.0	2022.5		1.0344	Ta(NN) ₅
2058.6	1990.2	2058.6, 2039.3, 2022.5, 2010.6, 1990.3	1.0344	Ta(NN) ₄
2035.9	1968.3	2035.4, 2014.3, 1988.5, 1969.0	1.0344	Ta(NN) ₃
1991.3	1925.0	1991.3, 1957.6, 1943.1, 1924.9	1.0344	Ta(NN) ₃
1978.7	1913.5	1978.7, 1934.8, 1913.5	1.0341	Ta(NN) ₂
1934.8	1870.9	1934.8, 1870.9	1.0342	Ta(NN)
1921.8	1859.4	1921.7, 1859.0	1.0336	Ta(NN) site

and Figure 1). The band shifts to 1875.5 cm^{-1} with $^{15}\text{N}_2$, giving a 1.0341 $^{14}\text{N}/^{15}\text{N}$ isotopic frequency ratio, which is characteristic of a N–N stretching vibration. The $^{14}\text{N}_2 + ^{15}\text{N}_2$ experiment reveals a clear 1939.5 and 1875.3 cm^{-1} mixed isotopic doublet (Figure 2); hence, one NN subunit is involved in these vibrations.²⁶ The 1939.5 cm^{-1} band is therefore assigned to the N–N stretching vibration of the Nb(NN) complex in solid neon, which is in accord with the previous tentative assignments in pure nitrogen (1965.2 cm^{-1})^{8a} and excess argon (1926 and 1931 cm^{-1}).^{8b} In the Ta + N_2 experiments, the absorption of the analogous Ta(NN) molecule has been observed at 1934.8 cm^{-1} in solid neon (Table 1 and Figure 3–4), which is in agreement with the previous 1947.6 cm^{-1} pure nitrogen tentative assignment to the Ta(NN) species.^{8a}

DFT calculations have been performed for the Nb(NN) and Ta(NN) molecules to support the above assignments. The Nb(NN) and Ta(NN) molecules are predicted to have a linear geometry with a $^6\Sigma^+$ and $^4\Sigma^+$ ground state (Figure 5), respectively, consistent with the previous theoretical calculations.^{8,11} For the Nb(NN) molecule, the scaled N–N stretching frequency

(1991.9 cm^{-1}) and the $^{14}\text{N}/^{15}\text{N}$ isotopic frequency ratio (1.0350) (Table 2) are consistent with the experimental values 1939.5 and 1.0341, respectively. Overall agreement between the experimental and calculated results has also been obtained for the Ta(NN) molecule (Table 2 and Figure 5).

M(NN)₂. In the Nb + N_2 experiments, the absorption at 2039.9 cm^{-1} appears during sample deposition, increases upon sample annealing, almost disappears after broad-band irradiation, and markedly recovers after further annealing to higher temperature (Table 1 and Figure 1). The band shifts to 1972.4 cm^{-1} with $^{15}\text{N}_2$, exhibiting isotopic frequency ratio ($^{14}\text{N}/^{15}\text{N}$, 1.0342) characteristic of N–N stretching vibration. As can be seen in Figure 2, a triplet isotopic pattern is observed in the mixed $^{14}\text{N}_2 + ^{15}\text{N}_2$ isotopic spectra, which indicates that two N_2 units are involved in the complex.²⁶ Accordingly, this band is assigned to the antisymmetric N–N stretching mode of the Nb(NN)₂ molecule. This band of Nb(NN)₂ appears to be a partially resolved doublet (Figure 1 and 2), which may be due to the N–N stretching vibration of this species in different matrix sites. The Nb(NN)₂ argon matrix counterpart was not identified in

TABLE 2: Comparison of Observed and Calculated IR Frequencies (in cm^{-1}) and Isotopic Frequency Ratios for the Products

species	observed		calculated	
	$\nu_{\text{N-N}}$	$^{14}\text{N}_2/^{15}\text{N}_2$	$\nu_{\text{N-N}}$ (intensity, mode) ^a	$^{14}\text{N}_2/^{15}\text{N}_2$
Nb(NN)	1939.5	1.0341	1991.9 (1032, σ)	1.0350
Nb(NN) ₂	2039.9	1.0342	2069.2 (2769, B ₂) 2128.3 (20, A ₁)	1.0350
Nb(NN) ₃	1949.3	1.0343	2040.0 (968, A ₁)	1.0350
	1998.8	1.0343	2077.6 (2280, B ₂) 2135.4 (16, A ₁)	1.0350
Nb(NN) ₄	2079.4	1.0341	2101.4 (0, B _{1g})	1.0350
			2108.1 (2072 \times 2, E _u) 2182.9 (0, A _{1g})	
Ta(NN)	1934.8	1.0343	1875.8 (792, σ)	1.0350
Ta(NN) ₂	1978.7	1.0341	2018.1 (2628, B ₂) 2103.2 (0, A ₁)	1.0350
Ta(NN) ₃	1991.3	1.0344	1974.5 (1070, A ₁)	1.0350
	2035.9	1.0344	2025.0 (2373, B ₂) 2090.0 (3, A ₁)	1.0350
Ta(NN) ₄	2058.6	1.0344	2058.9 (2336 \times 2, E _u) 2060.2 (0, B _{1g}) 2147.6 (0, A _{1g})	1.0350

^a Calculated frequencies are scaled by a factor of 0.9663;²⁵ intensities (in parentheses) are given in kilometers per mole.

TABLE 3: Energetics for Possible Reactions of Nb and Ta Atoms with N₂ Calculated at the B3LYP/6-311+G(d)-LANL2DZ Level

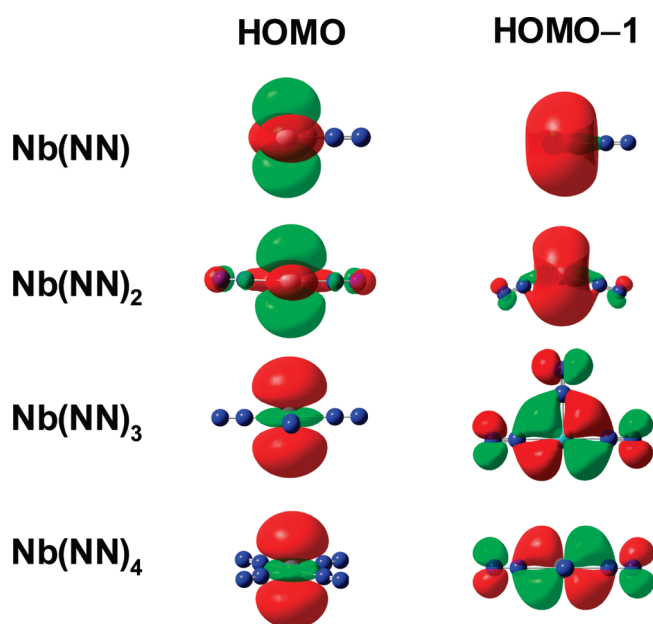
no.	reaction	reaction energy ^a (kcal/mol)
1	Nb(⁶ D) + N ₂ (¹ Σ_g^+) → NbNN(⁶ Σ^+)	-21.4
2	NbNN(⁶ Σ^+) + N ₂ (¹ Σ_g^+) → Nb(NN) ₂ (⁶ A ₁)	-18.0
3	Nb(NN) ₂ (⁶ A ₁) + N ₂ (¹ Σ_g^+) → Nb(NN) ₃ (⁴ B ₂)	-18.0
4	Nb(NN) ₃ (⁴ B ₂) + N ₂ (¹ Σ_g^+) → Nb(NN) ₄ (⁴ A _{1g})	-21.1
5	Ta(⁴ F) + N ₂ (¹ Σ_g^+) → TaNN(⁴ Σ^+)	-14.8
6	TaNN(⁴ Σ^+) + N ₂ (¹ Σ_g^+) → Ta(NN) ₂ (⁴ B ₁)	-16.1
7	Ta(NN) ₂ (⁴ B ₁) + N ₂ (¹ Σ_g^+) → Ta(NN) ₃ (⁴ B ₂)	-24.9
8	Ta(NN) ₃ (⁴ B ₂) + N ₂ (¹ Σ_g^+) → Ta(NN) ₄ (⁴ A _{1g})	-25.2

^a A negative value of energy denotes that the reaction is exothermic.

the previous experiments,⁸ but the Nb(CO)₂ molecule was observed at 1847.2 cm^{-1} in solid neon.^{22a}

The analogous feature with Ta and N₂ in neon appears during sample deposition at 1978.7 cm^{-1} , sharply increases upon sample annealing, almost disappears after broad-band irradiation, and recovers after further annealing to higher temperature (Table 1 and Figures 3 and 4). This band is assigned to the antisymmetric N–N stretching modes of the Ta(NN)₂ molecule on the basis of isotopic shift and splitting patterns.

B3LYP calculations predict the Nb(NN)₂ and Ta(NN)₂ molecules to have C_{2v} symmetry with a ⁶A₁ and ⁴B₁ ground electronic state (Figure 5), respectively, which are slightly lower in energy than the corresponding linear structures. Loss of one electron in the Nb(NN)₂ molecule results in a linear geometry.¹¹ For the Nb(NN)₂ molecule, the scaled antisymmetric N–N stretching frequency is predicted at 2069.2 cm^{-1} (Table 2), which is consistent with the experimental value (2039.9 cm^{-1}). The calculated band 2128.3 cm^{-1} with very low intensity (20 km/mol) is not readily observed, which is consistent with the absence of the symmetric N–N stretching vibration of the Nb(NN)₂ molecule from the present experiments. As summarized in Table 2, the calculated ¹⁴N/¹⁵N isotopic frequency ratio of 1.0350 is also in accord with the experimental value (1.0342). Similar results have been obtained for the Ta(NN)₂ molecule (Table 2 and Figure 5). This agreement between the experimental and calculated vibrational frequencies, relative

**Figure 6.** Molecular orbital depictions of the highest occupied molecular orbitals (HOMOs) and HOMO-1s of the niobium dinitrogen complexes.

absorption intensities, and isotopic shifts confirms the identifications of the Nb(NN)₂ and Ta(NN)₂ molecules from the matrix IR spectra.

M(NN)₃. In the reactions of laser-ablated Nb atoms with N₂, the 1998.8 and 1949.3 cm^{-1} bands weakly appear together during sample deposition, visibly increase on sample annealing, markedly decrease after broad-band irradiation, and recover after further annealing to higher temperature (Table 1 and Figure 1). The two bands shift to 1932.6 and 1884.6 cm^{-1} , respectively, in the ¹⁵N₂ experiment with exactly the same 1.0343 ¹⁴N/¹⁵N isotopic frequency ratio. In the ¹⁴N₂ + ¹⁵N₂ experiment, two sets of quartet bands, 1998.8/1983.3/1958.6/1932.5 and 1949.3/1929.5/1894.4/1884.6 cm^{-1} , have been observed (Table 1 and Figure 2), which is reminiscent of the Rh(NN)₃ and Fe(NN)₃ complex in solid neon.^{27,28} Accordingly, these bands are suitable for the N–N stretching vibration of the Nb(NN)₃ molecule. The corresponding N–N stretching frequencies of the analogous Ta(NN)₃ product have been observed at 2035.9 and 1991.3 cm^{-1}

in solid neon (Table 1 and Figures 3 and 4). The matrix counterparts for $\text{Nb}(\text{NN})_3$ and $\text{Ta}(\text{NN})_3$ were not identified in the previous argon and pure nitrogen experiments.⁸

The $\text{Nb}(\text{NN})_3$ and $\text{Ta}(\text{NN})_3$ assignments are strongly supported by the DFT frequency calculations (Table 2). The $\text{Nb}(\text{NN})_3$ and $\text{Ta}(\text{NN})_3$ molecules are predicted to be T-shaped with a ${}^4\text{B}_2$ ground electronic state (Figure 5), similar to the $\text{Rh}(\text{NN})_3$ molecule.²⁷ Previously, B3LYP calculations predicted the $\text{Nb}^+(\text{N}_2)_3$ molecule to have a ${}^5\text{A}_1$ ground state with a C_{2v} symmetry.¹¹ In the $\text{Nb}(\text{NN})_3$ molecule, as an example, three N–N stretching modes are calculated at 2135.4 cm^{-1} (16 km/mol, A_1), 2077.6 cm^{-1} (2280 km/mol, B_2), and 2040.0 cm^{-1} (968 km/mol, A_1) (Table 2). The band at 2135.4 cm^{-1} with very low intensity (16 km/mol) is not readily observed, which is consistent with the absence of this N–N stretching vibration of the $\text{Nb}(\text{NN})_3$ molecule from the present experiments. The calculated bands 2077.6 and 2040.0 cm^{-1} are consistent with the experimental frequencies 1998.8 and 1949.3 cm^{-1} , respectively. As listed in Table 2, the calculated ${}^{14}\text{N}_2/{}^{15}\text{N}_2$ isotopic frequency ratio of 1.0350 is also in accord with the experimental observation (1.0343). Similar results have also been obtained for the $\text{Ta}(\text{NN})_3$ molecule (Table 2 and Figure 5).

$M(\text{NN})_4$. The 2079.4 cm^{-1} band with Nb and N_2 in neon weakly appears upon sample annealing, visibly increases after broad-band irradiation, and slightly increases after further annealing to higher temperature (Table 1 and Figure 1). This band shifts to 2010.8 cm^{-1} with ${}^{15}\text{N}_2$, exhibiting an isotopic frequency ratio (${}^{14}\text{N}/{}^{15}\text{N}$, 1.0341) characteristic of N–N stretching vibration. As can be seen in Figure 2, a quintet isotopic pattern has been observed in the mixed ${}^{14}\text{N}_2 + {}^{15}\text{N}_2$ experiment, which is the characteristic feature for the triply degenerate mode of a tetrahedral species.²⁶ This band is therefore assigned to the N–N stretching vibration of the $\text{Nb}(\text{NN})_4$ molecule in solid neon, which is 6.9 cm^{-1} above the argon matrix value.^{8a} It is noted that previous gas phase experiments observed the N–N stretching vibration of $\text{Nb}^+(\text{N}_2)_4$ at 2264 cm^{-1} .¹¹ Similar neon matrix experiments of Ta and N_2 give the absorption of the analogous $\text{Ta}(\text{NN})_4$ molecule at 2058.6 cm^{-1} (Table 1 and Figures 3 and 4). This band is in accord with previous 2040.9 cm^{-1} assignment to $\text{Ta}(\text{NN})_4$ in pure nitrogen.^{8a}

Our DFT calculations predict the $\text{Nb}(\text{NN})_4$ and $\text{Ta}(\text{NN})_4$ molecules to have D_{4h} symmetry with a ${}^4\text{A}_{1g}$ ground electronic state (Figure 5), in accord with the previous report for a square-planar D_{4h} $\text{Nb}(\text{NN})_4$.^{8b} The $\text{Nb}^+(\text{N}_2)_4$ complex was also predicted to have D_{4h} symmetry with a ${}^5\text{B}_{2g}$ ground state in the previous B3LYP calculations.¹¹ For the $\text{Nb}(\text{NN})_4$ molecule, the scaled antisymmetric N–N stretching frequency is predicted at 2108.1 cm^{-1} (Table 2), only 28.7 cm^{-1} lower than the present neon matrix value. As summarized in Table 2, the calculated ${}^{14}\text{N}_2/{}^{15}\text{N}_2$ isotopic frequency ratio of 1.0350 is also in accord with the experimental value (1.0341). Similar results have been obtained for the $\text{Ta}(\text{NN})_4$ molecule (Table 2 and Figure 5). These agreements of the $\text{Nb}(\text{NN})_4$ and $\text{Ta}(\text{NN})_4$ molecules are supported by the agreement between the experimental and the calculated vibrational frequencies and isotopic shifts.

$M(\text{NN})_{5,6}$. In the Nb + N_2 experiments, the 2149.4 , 2130.0 , 2100.1 , and 2049.4 cm^{-1} bands appear after broad-band irradiation, slightly increase on sample annealing, and show N–N stretching frequency ratios (Table 1). The mixed isotopic structures for these bands were not well-resolved because of band overlap and isotopic dilution. Compared with the previous Nb + N_2 system in pure nitrogen, for which the bands at 2140.2 and 2134.8 cm^{-1} were assigned to the $\text{Nb}(\text{NN})_6$ molecule,^{8a} the 2149.4 and 2130.0 cm^{-1} bands in excess neon are probably due

to the $\text{Nb}(\text{NN})_6$ molecule. The 2100.1 and 2049.4 cm^{-1} may be due to the N–N stretching vibrations of $\text{Nb}(\text{NN})_5$ and $(\text{NN})_x\text{Nb}(\text{NN})$, respectively. Analogous potential $\text{Ta}(\text{NN})_5$ and $\text{Ta}(\text{NN})_6$ molecules have been observed at 2092.0 and 2110.0 cm^{-1} in the present experiments (Table 1). The 2110.0 cm^{-1} band is in accord with previous 2106.4 cm^{-1} assignments to $\text{Ta}(\text{NN})_6$ in an argon matrix.^{8a}

Reaction Mechanism. At the present experimental conditions, laser-ablated niobium and tantalum atoms react with N_2 in the excess neon matrixes to produce the binary metal dinitrogen complexes $M(\text{NN})_x$ ($M = \text{Nb, Ta}$; $x = 1-4$). The absorptions of the metal dinitrogen complexes increase on annealing, suggesting the reactions to form these species are spontaneous. The $\text{Nb}(\text{NN})$ and $\text{Ta}(\text{NN})$ molecules appear during sample deposition and increase upon annealing (Figures 1 and 3 and Table 1), suggesting that these products may be formed from the reactions of niobium and tantalum atoms with N_2 (Table 3, reactions 1 and 5). Higher metal dinitrogen complexes may be formed via the N_2 addition (reactions 2–4 and 6–8). As can be seen in Table 3 (reactions 1–8), all association reactions are predicted to be exothermic (-14.8 to -25.2 kcal/mol), in agreement with the experimental observations.

As illustrated in Figure 6, the highest occupied molecular orbitals (HOMOs) in the $\text{Nb}(\text{NN})$ and $\text{Nb}(\text{NN})_2$ are of δ -type with the contribution mainly from the Nb 4d atomic orbitals, whereas the HOMO-1s are of σ -type and are largely Nb 5s and 4d in character. In addition, the HOMOs in $\text{Nb}(\text{NN})_3$ and $\text{Nb}(\text{NN})_4$ are largely Nb 5s and 4d in character and are nonbonding. The degenerate HOMO-1s in $\text{Nb}(\text{NN})_3$ and $\text{Nb}(\text{NN})_4$ are the M–N π bonding orbitals, which are responsible for the stability of these metal dinitrogen complexes. Such bonding features hold true for the tantalum dinitrogen complexes.

Conclusions

Niobium and tantalum dinitrogen complexes $M(\text{NN})_x$ ($M = \text{Nb, Ta}$; $x = 1-4$) have been prepared by the reactions of laser-ablated niobium and tantalum atoms with N_2 in excess neon. In the niobium experiments, the absorptions at 1939.5 , 2039.9 , 1998.8 , 1949.3 , and 2079.4 cm^{-1} are assigned to the N–N stretching vibrations of the $\text{Nb}(\text{NN})$, $\text{Nb}(\text{NN})_2$, $\text{Nb}(\text{NN})_3$, and $\text{Nb}(\text{NN})_4$ molecules, respectively, on the basis of the isotopic shifts and mixed isotopic splitting patterns. Analogous $\text{Ta}(\text{NN})_x$ ($x = 1-4$) products have been observed in the tantalum experiments. DFT calculations have been performed, which lend support to the experimental assignments of the matrix infrared spectra.

Acknowledgment. This work was supported by AIST and a Grant-in-Aid for Scientific Research (B) (Grant No. 17350012) from the Ministry of Education, Culture, Sports, Science and Technology (MEXT) of Japan. Z.-H.L. acknowledges JASSO and Kobe University for an Honors Scholarship.

References and Notes

- (1) Cotton, F. A.; Wilkinson, G.; Murillo, C. A.; Bochmann, M. *Advanced Inorganic Chemistry*, 6th ed.; Wiley: New York, 1999.
- (2) (a) Howard, J. B.; Rees, D. C. *Chem. Rev.* **1996**, *96*, 2965. (b) Burgess, N. K.; Lowe, D. J. *Chem. Rev.* **1996**, *96*, 2983.
- (3) (a) Pool, J. A.; Lobkovsky, E.; Chirik, P. J. *Nature* **2004**, *427*, 527. (b) Houlton, B. Z.; Wang, Y. P.; Vitousek, P. M.; Field, C. B. *Nature* **2008**, *454*, 327. (c) Fryzuk, M. D.; Love, J. B.; Rettig, S. J.; Young, V. G. *Science* **1997**, *275*, 1445. (d) Yandulov, D. V.; Schrock, R. R. *Science* **2003**, *301*, 76.
- (4) Allen, A. D.; Senoff, C. V. *Chem. Commun.* **1965**, 621.
- (5) (a) Himmel, H. J.; Reiher, M. *Angew. Chem., Int. Ed.* **2006**, *45*, 6264. (b) MacLachlan, E. A.; Fryzuk, M. D. *Organometallics* **2006**, *25*, 1530. (c) Gambarotta, S.; Scott, J. *Angew. Chem., Int. Ed.* **2004**, *43*, 5298.

- (d) MacKay, B. A.; Fryzuk, M. D. *Chem. Rev.* **2004**, *104*, 385. (e) Himmel, H. J.; Downs, A. J.; Greene, T. M. *Chem. Rev.* **2002**, *102*, 4191. (f) Hidai, M.; Mizobe, Y. *Chem. Rev.* **1995**, *95*, 1115.
- (6) Shan, H.; Yang, Y.; James, A. J.; Sharp, P. R. *Science* **1997**, *275*, 1460.
- (7) Andrews, L.; Bare, W. D.; Chertihin, G. V. *J. Phys. Chem. A* **1997**, *101*, 8417.
- (8) (a) Zhou, M. F.; Andrews, L. *J. Phys. Chem. A* **1998**, *102*, 9061. (b) Green, D. W.; Hodges, R. V.; Gruen, D. M. *Inorg. Chem.* **1976**, *15*, 970.
- (9) Parrish, S. H.; Van Zee, R. J.; Weltner, W., Jr. *J. Phys. Chem. A* **1999**, *103*, 1025.
- (10) Pillai, E. D.; Jaeger, T. D.; Duncan, M. A. *J. Phys. Chem. A* **2005**, *109*, 3521.
- (11) Pillai, E. D.; Jaeger, T. D.; Duncan, M. A. *J. Am. Chem. Soc.* **2007**, *129*, 2297.
- (12) Avenier, P.; Taoufik, M.; Lesage, A.; Solans-Monfor, X.; Baudouin, A.; de Mallmann, A.; Veyre, L.; Basset, J. M.; Eisenstein, O.; Emsley, L.; Quadrelli, E. A. *Science* **2007**, *317*, 1056.
- (13) (a) Mwakapumba, J.; Ervin, K. M. *Int. J. Mass Spectrom. Ion Processes* **1997**, *161*, 161. (b) Berces, A.; Hackett, P. A.; Lian, L.; Mitchell, S. A.; Rayner, D. M. *J. Chem. Phys.* **1998**, *108*, 13. (c) An, B.; Xu, M.; Fukuyama, S.; Yokogawa, K. *Phys. Rev. B* **2006**, *73*, 205401. (d) Franchy, R.; Bartke, T. U. *Surf. Sci.* **1995**, *322*, 95. (e) Li, J.; Li, S. H. *Angew. Chem., Int. Ed.* **2008**, *47*, 8040. (f) Sellers, H. J. *J. Phys. Chem.* **1990**, *94*, 1338. (g) Berces, A.; Mitchell, S. A.; Zgierski, M. Z. *J. Phys. Chem. A* **1998**, *102*, 6340.
- (14) Zhou, M. F.; Andrews, L.; Bauschlicher, C. W., Jr. *Chem. Rev.* **2001**, *101*, 1931. (b) Andrews, L.; Citra, A. *Chem. Rev.* **2002**, *102*, 885. (c) Xu, Q. *Coord. Chem. Rev.* **2002**, *231*, 83. (d) Wang, G. J.; Zhou, M. F. *Int. Rev. Phys. Chem.* **2008**, *27*, 1. (f) Gong, Y.; Zhou, M. F.; Andrews, L. *Chem. Rev.* **2009**, *109*, 6765, and references therein.
- (15) (a) Li, J.; Bursten, B. E.; Liang, B.; Andrews, L. *Science* **2002**, *295*, 2242. (b) Andrews, L.; Wang, X. *Science* **2003**, *299*, 2049. (c) Zhou, M. F.; Zhang, L. N.; Qin, Q. Z. *J. Am. Chem. Soc.* **2000**, *122*, 4483. (d) Zhou, M. F.; Dong, J.; Zhang, L. N.; Qin, Q. Z. *J. Am. Chem. Soc.* **2001**, *123*, 135. (e) Zhou, M. F.; Zeng, A. H.; Wang, Y.; Kong, Q. Y.; Wang, Z. X.; Schleyer, P. v. R. *J. Am. Chem. Soc.* **2003**, *125*, 11512. (f) Zhou, M. F.; Zhao, Y. Y.; Gong, Y.; Li, J. *J. Am. Chem. Soc.* **2006**, *128*, 2504. (g) Wang, G. J.; Gong, Y.; Chen, M. H.; Zhou, M. F. *J. Am. Chem. Soc.* **2006**, *128*, 5974. (h) Zhou, M. F.; Jin, X.; Gong, Y.; Li, J. *Angew. Chem., Int. Ed.* **2007**, *46*, 2911. (i) Wang, X.; Andrews, L. *J. Am. Chem. Soc.* **2008**, *130*, 6766.
- (16) (a) Zhou, M. F.; Tsumori, N.; Li, Z.; Fan, K.; Andrews, L.; Xu, Q. *J. Am. Chem. Soc.* **2002**, *124*, 12936. (b) Zhou, M. F.; Xu, Q.; Wang, Z.; Schleyer, P. v. R. *J. Am. Chem. Soc.* **2002**, *124*, 14854. (c) Jiang, L.; Xu, Q. *J. Am. Chem. Soc.* **2005**, *127*, 42. (d) Xu, Q.; Jiang, L.; Tsumori, N. *Angew. Chem., Int. Ed.* **2005**, *44*, 4338. (e) Jiang, L.; Xu, Q. *J. Am. Chem. Soc.* **2005**, *127*, 8906. (f) Teng, Y. L.; Kohyama, M.; Haruta, M.; Xu, Q. *J. Chem. Phys.* **2009**, *130*, 134511.
- (17) (a) Burkholder, T. R.; Andrews, L. *J. Chem. Phys.* **1991**, *95*, 8697. (b) Hassanzadeh, P.; Andrews, L. *J. Chem. Phys.* **1992**, *96*, 9177. (c) Jiang, L.; Xu, Q. *J. Chem. Phys.* **2005**, *122*, 034505.
- (18) Frisch, M. J.; Trucks, G. W.; Schlegel, H. B.; Scuseria, G. E.; Robb, M. A.; Cheeseman, J. R.; Montgomery, J. A., Jr.; Vreven, T.; Kudin, K. N.; Burant, J. C.; Millam, J. M.; Iyengar, S. S.; Tomasi, J.; Barone, V.; Mennucci, B.; Cossi, M.; Scalmani, G.; Rega, N.; Petersson, G. A.; Nakatsuji, H.; Hada, M.; Ehara, M.; Toyota, K.; Fukuda, R.; Hasegawa, J.; Ishida, M.; Nakajima, T.; Honda, Y.; Kitao, O.; Nakai, H.; Klene, M.; Li, X.; Knox, J. E.; Hratchian, H. P.; Cross, J. B.; Bakken, V.; Adamo, C.; Jaramillo, J.; Gomperts, R.; Stratmann, R. E.; Yazyev, O.; Austin, A. J.; Cammi, R.; Pomelli, C.; Ochterski, J. W.; Ayala, P. Y.; Morokuma, K.; Voth, G. A.; Salvador, P.; Dannenberg, J. J.; Zakrzewski, V. G.; Dapprich, S.; Daniels, A. D.; Strain, M. C.; Farkas, O.; Malick, D. K.; Rabuck, A. D.; Raghavachari, K.; Foresman, J. B.; Ortiz, J. V.; Cui, Q.; Baboul, A. G.; Clifford, S.; Cioslowski, J.; Stefanov, B. B.; Liu, G.; Liashenko, A.; Piskorz, P.; Komaromi, I.; Martin, R. L.; Fox, D. J.; Keith, T.; Al Laham, M. A.; Peng, C. Y.; Nanayakkara, A.; Challacombe, M.; Gill, P. M. W.; Johnson, B.; Chen, W.; Wong, M. W.; Gonzalez, C.; Pople, J. A. *Gaussian 03*, revision B.04; Gaussian, Inc.: Pittsburgh, PA, 2003.
- (19) (a) Lee, C.; Yang, W.; Parr, R. G. *Phys. Rev. B* **1988**, *37*, 785. (b) Becke, A. D. *J. Chem. Phys.* **1993**, *98*, 5648.
- (20) (a) McLean, A. D.; Chandler, G. S. *J. Chem. Phys.* **1980**, *72*, 5639. (b) Krishnan, R.; Binkley, J. S.; Seeger, R.; Pople, J. A. *J. Chem. Phys.* **1980**, *72*, 650. (c) Frisch, M. J.; Pople, J. A.; Binkley, J. S. *J. Chem. Phys.* **1984**, *80*, 3265.
- (21) Hay, P. J.; Wadt, W. R. *J. Chem. Phys.* **1985**, *82*, 299.
- (22) (a) Zhou, M. F.; Andrews, L. *J. Phys. Chem. A* **1999**, *103*, 7785. (b) Teng, Y. L.; Xu, Q. *J. Phys. Chem. A* **2008**, *112*, 3607. (c) Lu, Z. H.; Jiang, L.; Xu, Q. *J. Chem. Phys.* **2009**, *131*, 034512. (d) Lu, Z. H.; Xu, Q. *J. Phys. Chem. Chem. Phys.* **2010**, DOI: 10.1039/c000398k.
- (23) (a) Zhai, H. J.; Kiran, B.; Dai, B.; Li, J.; Wang, L. S. *J. Am. Chem. Soc.* **2005**, *127*, 12098. (b) Huang, W.; Bulusu, S.; Pal, R.; Zeng, X. C.; Wang, L. S. *J. Chem. Phys.* **2009**, *131*, 234305. (c) Wang, Y. L.; Zhai, H. J.; Xu, L.; Li, J.; Wang, L. S. *J. Phys. Chem. A* **2010**, *114*, 1247.
- (24) (a) Ono, Y.; Taketsugu, T. *J. Chem. Phys.* **2004**, *120*, 6035. (b) Taketsugu, Y.; Noro, T.; Taketsugu, T. *Chem. Phys. Lett.* **2010**, *484*, 139.
- (25) (a) Scott, A. P.; Radom, L. *J. Phys. Chem.* **1996**, *100*, 16502. (b) Ohzdam, Z.; Yurdakul, M.; Yurdakul, S. *Vib. Spectrosc.* **2007**, *43*, 335.
- (26) Darling, J. H.; Ogden, J. S. *J. Chem. Soc., Dalton Trans.* **1972**, 2496.
- (27) Wang, X.; Andrews, L. *J. Phys. Chem. A* **2002**, *106*, 2457.
- (28) Lu, Z. H.; Jiang, L.; Xu, Q. *J. Phys. Chem. A* **2010**, *114*, 2157.